Journal of Coordination Chemistry

ISSN: 0095-8972 (Print) 1029-0389 (Online) Journal homepage: http://www.tandfonline.com/loi/gcoo20

Iron(IV) or iron(V)? Heterolytic or free radical? Oxidation pathways of a TAML activator in acetonitrile at −40 °C

Matthew R. Mills, Abigail E. Burton, Dylan I. Mori, Alexander D. Ryabov & Terrence J. Collins

To cite this article: Matthew R. Mills, Abigail E. Burton, Dylan I. Mori, Alexander D. Ryabov & Terrence J. Collins (2015) Iron(IV) or iron(V)? Heterolytic or free radical? Oxidation pathways of a TAML activator in acetonitrile at −40 °C, Journal of Coordination Chemistry, 68:17-18, 3046-3057, DOI: 10.1080/00958972.2015.1073270

To link to this article: http://dx.doi.org/10.1080/00958972.2015.1073270

Accepted author version posted online: 20 Jul 2015.
Published online: 14 Aug 2015.

Submit your article to this journal

Article views: 105

View related articles

View Crossmark data

Full Terms & Conditions of access and use can be found at
http://www.tandfonline.com/action/journalInformation?journalCode=gcoo20

Download by: [Mizoram University] **Date:** 28 December 2015, At: 14:40

Journal of Coordination Chemistry, 2015
Vol. 68, Nos. 17–18, 3046–3057, http://dx.doi.org/10.1080/00958972.2015.1073270

Taylor & Francis
Taylor & Francis Group

Iron(IV) or iron(V)? Heterolytic or free radical? Oxidation pathways of a TAML activator in acetonitrile at −40 °C

MATTHEW R. MILLS, ABIGAIL E. BURTON, DYLAN I. MORI, ALEXANDER D. RYABOV* and TERRENCE J. COLLINS*

Department of Chemistry, Carnegie Mellon University, Pittsburgh, PA, USA

(*Received 3 April 2015; accepted 10 July 2015*)

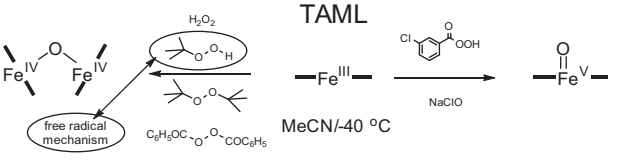

The oxidation of TAML complex $[Fe^{III}\{C_6H_4\text{-}1,2\text{-}(NCOCMe_2NCO)_2CMe_2\}OH_2]^-$ (**1**) by various oxidants is explored in MeCN with 0.2% water at −40 °C, where the iron(V)oxo complex is stable enough for reliable spectral identification. The iron(V)oxo state is achieved using NaClO even faster than in the case of previously explored *m*-chloroperoxybenzoic acid. In contrast, H_2O_2 and organic peroxides (benzoyl peroxide, *tert*-butylperoxide, and *tert*-butylhydroperoxide) all convert **1** into the corresponding diiron(IV)-μ-oxo dimer (**2**) under the same conditions. The latter does not form when $(NH_4)_2[Ce(NO_3)_6]$ is employed and the Fe^{IV} product obtained does not seem to contain an oxo moiety. In contrast to all other oxidants, the conversion of **1** by ^{t}BuOOH into **2** is characterized by non-conventional kinetics, and therefore this reaction was explored in some detail. The evidence is presented that this light-, O_2-, TEMPO-, and base-dependent reaction is a free radical process under the conditions used.

Keywords: Iron complex; High-valent; TAML; *tert*-Butylhydroperoxide; Kinetics; Mechanism

Downloaded by [Mizoram University] at 14:40 28 December 2015

1. Introduction

Iron complexes in oxidation states three and above play key roles in a multitude of enzymatic and catalytic chemical oxidations [1–11]. Various mechanistic aspects of the formation of such high-valent iron species have been a subject of careful investigation by multiple researchers, including van Eldik, to whom this issue is devoted [12–16]. Noticeable attention has been paid recently to TAML activators of peroxides [17–22]. These iron (III) complexes in the tetraamido macrocyclic environment prove to be truly exceptional in two important aspects. In water, they are remarkable functional replicas of peroxidase enzymes capable of performing a vast array of degradations of environmental pollutants, including endocrine disruptors [23–28]. In organic solvents, the unique features of TAMLs

*Corresponding authors. Email: ryabov@andrew.cmu.edu (A.D. Ryabov); tc1u@andrew.cmu.edu (T.J. Collins)

© 2015 Taylor & Francis

allow one to spectroscopically and crystallographically characterize a broad spectrum of oxidized iron species which could be considered as plausible participants of the catalytic cycle in aqueous solutions. The most significant among these are the Fe^{III} superoxo complex, $Fe^{III}O_2$ made from iron(III) and KO_2 at −5 °C in MeCN [29], the $Fe^{IV}OFe^{IV}$ μ-oxo dimer which is generated by O_2 from iron(III) in non-coordinating solvents such as CH_2Cl_2 under ambient conditions [30], and the $Fe^{V}O$ complex which is produced using *m*-chloroperoxybenzoic acid (*m*CPBA) at −40 °C in MeCN [31]. TAML complexes are used as catalysts in synthetically valuable transformations using different oxidizing agents under various conditions [32–36]. As a rule, the synthetic reports are concluded by postulated reaction mechanisms, in which high oxidation states of iron, often Fe^{V}, are proposed irrespective of the reaction conditions and the oxidizing agent used. In our experience, however, the Fe^{V} oxidation state is not attained by the most commonly used TAML activator **1** (chart 1) in all instances. Consequently, we have been challenged by this question, which oxidants can convert the Fe^{III} species **1** into its Fe^{V} form **3**, and which oxidants yield the Fe^{IV} form **2**? Compounds **2** and **3** have distinct UV–vis spectral signatures at −40 °C in MeCN [32], which allowed unambiguous assignment of the products formed in the presence of a series of oxidants which are summarized in table 1. While following the product formation in the presence of ^{t}BuOOH, which converts **1** into **2** (III → IV oxidation), we noticed that the reaction dynamics is strikingly different compared to all other oxidants used. Therefore, we have also collected a significant amount of kinetic data for the **1** → **2** oxidation by ^{t}BuOOH, which allowed us to conclude that, in contrast to other oxidations, this transformation occurs via a free radical mechanism.

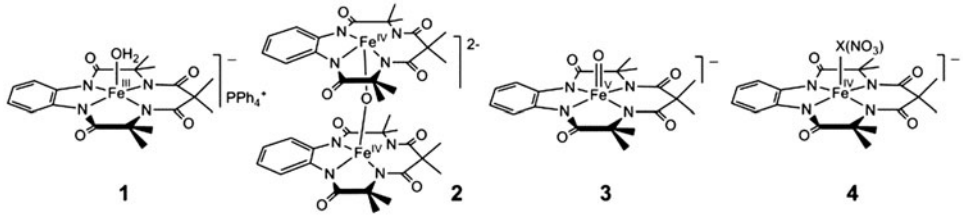

Chart 1. TAML derivatives discussed in this work.

Table 1. Final products obtained upon reaction of **1** with various oxidants. Conditions for all reactions: [**1**] = 1.0×10^{-4} M in acetonitrile with 0.2% water at −40 °C.

Oxidant	Amount, M	Reaction time	Product and yield	Reference
*m*CPBA	1×10^{-4}	**2**: 100 s **3**: 60 min	**2**: >99% **3**: >95%	[31, 32]
$NaClO_4$	2×10^{-4}	**2**: 5 s **3**: 30 min	**2**: >99% **3**: >95%	This work
Benzoyl peroxide	5×10^{-3}	**2**: 84 min	90%	This work
tert-Butylperoxide	6×10^{-2}	**2**: 185 min	89%	This work
Hydrogen peroxide	1×10^{-2}	**2**: 83 min	83%	This work
tert-Butylhydroperoxide	7.3×10^{-3}	**2**: 20 min	89%	This work
$(NH_4)_2[Ce(NO_3)_6]$	1×10^{-4}	**4**: 10 s	~100%[a]	[38]

[a]Calculated using $\varepsilon = 5160\ M^{-1}\ cm^{-1}$ at 533 nm from Ref. [38] for the ring-di-methoxy analog of **1**.

Downloaded by [Mizoram University] at 14:40 28 December 2015

2. Experimental

2.1. *Materials and methods*

Complex **1** was prepared from the corresponding sodium salt (GreenOx, Inc.) by the addition of PPh_4Cl to the aqueous solution as previously described, causing the precipitation of **1** [30]. The resulting product was recrystallized from 50% methanol/water. Anhydrous ^{t}BuOOH in toluene was prepared from 70% aqueous ^{t}BuOOH (Aldrich) as described elsewhere [37]. The additives, 2,2,6,6-tetramethylpiperidine (tmpp, ≥ 99%) and 18-crown-6, which was used to solubilize potassium *tert*-butoxide, were purchased from Aldrich. Glacial acetic acid (certified ACS grade) was purchased from Fisher. Potassium *tert*-butoxide was purchased from Strem Chemicals and sublimed in vacuo. 1,8-Bis (dimethylamino)naphthalene was purchased from Sigma and recrystallized three times from ethanol. Sodium bis(trimethylsilyl)amide (98%), 1,4–diazabicyclo[2.2.2]octane (dabco), ^{t}BuOH (99.5%), and (2,2,6,6-tetramethylpiperidin-1-yl)oxy (tempo, 98%) were purchased from Acros. Dabco was purified by sublimation in vacuo. Triethylamine was distilled over calcium hydride. Acetonitrile was dried using a SciMarco solvent dispensing system. UV–vis spectroscopy was performed using an Agilent 8453 instrument equipped with a liquid nitrogen-cooled cryostat setup from UNISOKU Scientific Instruments, Japan. All reactions were performed at −40 °C. The ^{1}H NMR spectra were registered using Bruker Avance 300 and Bruker Avance III 500 MHz NMR spectrometers.

2.2. *Kinetic studies*

Unless otherwise noted, water and acetonitrile stock solutions of **1** and additive, if necessary, were added to a quartz cuvette with a stir bar and diluted with acetonitrile. This solution was allowed to cool to −40 °C for 5 min before ^{t}BuOOH was injected. The final volume of all samples was 2 mL. The formation of **2** was monitored by UV–vis spectroscopy at 708 nm, which is the isosbestic point between **2** and **3** under the conditions selected. Unless otherwise noted, spectra were recorded every 2 s. Concentration of **2** was calculated using the previously determined extinction coefficient of 6280 M^{-1} cm^{-1} at 708 nm [32]. All reported rates are mean values of at least three measurements. Kinetic data in the absence of O_2 were obtained by preparing stock solutions of reagents in acetonitrile which had been subjected to three freeze–pump–thaw cycles. The reaction mixtures were prepared by adding appropriate volumes of deoxygenated stock solutions into a quartz cuvette fitted with a screw top cap and replaceable septum which had been purged with argon. The solution was diluted to the required volume with deoxygenated acetonitrile and the reaction conducted as described previously.

2.3. *^{1}H NMR studies*

Due to the fact that **1** is paramagnetic, ^{1}H NMR experiments were performed by adding **1** to initiate the reaction. The reaction mixture was prepared by dissolving ^{t}BuOOH in deuterated acetonitrile to achieve the desired concentration. This sample was analyzed by ^{1}H NMR and the shimming file was saved for analysis of the next sample. This solution was then poured into a quartz cuvette and inserted into the low-temperature apparatus and allowed to cool to −40 °C. The reaction was initiated by addition of **1** in deuterated acetonitrile and monitored as described in section 2.2. Upon completion of that reaction (as deter-

Downloaded by [Mizoram University] at 14:40 28 December 2015

mined by a leveling-off of the UV–vis trace at 708 nm), approximately 1 mL of the reaction mixture was pipetted into a chilled NMR tube, immediately placed in liquid nitrogen and frozen. This sample was kept in liquid nitrogen until analysis by ^{1}H NMR. Then, it was removed from the liquid nitrogen and allowed to warm just enough for the frozen condensation on the tube to melt and be wiped off. It was then analyzed by NMR without locking or shimming using the shim file from the previously prepared sample. Data were analyzed using a Bruker TopSpin 3.0 software.

3. Results and discussion

3.1. *The oxidation state of iron in the product is determined by the oxidant*

As mentioned in section 1, the UV–vis spectra of **2** and **3** produced from **1** in the presence of *m*CPBA as oxidant are sufficiently different for unambiguous assignments [32]. Therefore, it was relatively easy to specify the nature of the product formed from **1** and different oxidants shown in table 1 in wet MeCN at −40 °C. At such low temperature, the Fe^{V} species **3** is appropriately stable [32] and, if formed, could be reliably identified. In this work, the only oxidant beside *m*CPBA to produce **3** was NaClO. When 2 equivalents of this oxidant were added to **1**, the spectrum of intermediate iron(IV) complex **2** was observed within just 5 s and then transformed to the spectrum of iron(V) complex **3** in a matter of 30 min (figure 1). The spectra of **2** and **3** were identical to those reported elsewhere [32], which were observed upon reaction of **1** and *m*CPBA. In particular, **2** formed from **1** and NaClO revealed maxima at 435, 830, and 1050 nm; **3** at 447 and 630 nm with the isosbestic points between **2** and **3** at 708 nm. In contrast, regardless of their relative amount, none of the organic oxidants studied converted iron(III) to iron(V), only producing iron(IV) species in the form of **2**. Similar chemistry was observed for H_2O_2. In the case of

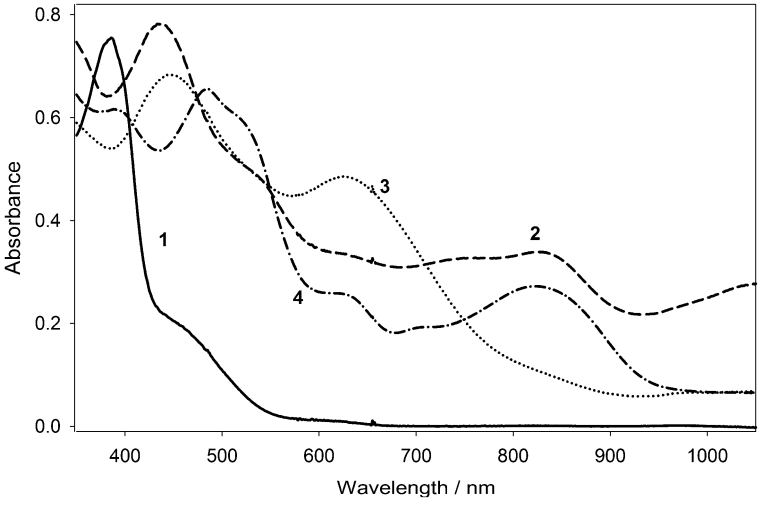

Figure 1. Spectra of **1** and the products of its oxidation by NaClO (2.0×10^{-4} M) **2** and **3** and by $(NH_4)_2[Ce(NO_3)_6]$ (1.0×10^{-4} M) **4**. Conditions: [**1**] 1.0×10^{-4} M in acetonitrile with 0.2% water at −40 °C.

Downloaded by [Mizoram University] at 14:40 28 December 2015

Downloaded by [Mizoram University] at 14:40 28 December 2015

^{t}BuOOH, we have noticed that the spectrum of **2** formed changes slightly with time and the changes could be associated with the accumulation of traces of **3**. However, attempts to increase the yield of **3** by increasing the loadings of ^{t}BuOOH or adding multiple aliquots were unsuccessful, and therefore we conclude that the oxidation state V of TAML derived from **1** cannot be reached under these conditions using H_2O_2 and organic peroxides, despite an excess of the oxidants, and the reactions lead to the Fe^{IV} species in the form of **2**. It is important to note that H_2O_2 and organic peroxides studied produced identical UV–vis spectra of the Fe^{IV} μ-oxo dimer **2** as shown in figure 1.

The oxidation of **1** by strong inorganic oxidant $(NH_4)_2[Ce(NO_3)_6]$ does not afford either **2** or **3**. The spectrum in figure 1 generated in this case differs from those of **2** or **3** revealing maxima at 485 and 825 nm, and the lack of strong absorption around 1050 nm, which is diagnostic of the presence of the Fe^{IV}–O–Fe^{IV} unit. The products obtained from Fe^{III} TAMLs and $(NH_4)_2[Ce(NO_3)_6]$ in organic solvents have been explored in detail in the 90s and identified by X-ray crystallography as the monomeric five-coordinate axially ligated Fe^{IV} species [38]. This allowed us to hypothesize that the same type of species is produced from **1** and Ce^{IV} at −40° and ascribe its structure such as **4**. Thus, the high-valent oxygen-ligated (μ-oxo or oxo) iron TAML species produced in MeCN at −40° C seem to stem from the oxidants incorporating active oxygen atoms.

Though just a few oxidants convert Fe^{III} TAML **1** into the Fe^{V} state, the Fe^{IV} state is reachable for all oxidants included in table 1. Therefore, it was interesting to compare their relative efficacy in promoting the $Fe^{III} \rightarrow Fe^{IV}$ conversions which result in the formation of the μ-oxo dimer **2**. The data for the comparison are shown in figure 2.

Sodium hypochlorite turned out to be so reactive that a separate timescale was constructed for this oxidant (top *x*-axis in figure 2), though its concentration was the lowest.

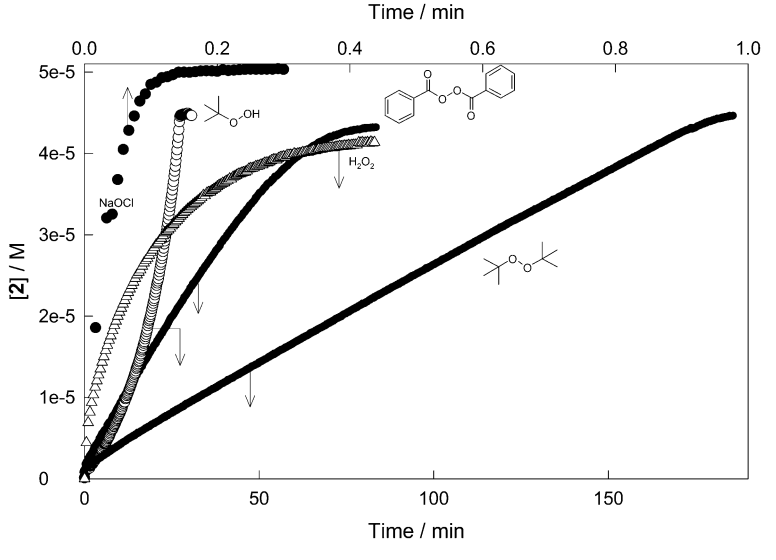

Figure 2. Kinetic traces for the $Fe^{III} \rightarrow Fe^{IV}$ conversions to form **2** in the presence of selected oxidants. Conditions: MeCN with 0.2% H_2O, −40 °C, [**1**] 1×10^{-4} M, [benzoyl peroxide] 5×10^{-3} M, [*tert*-butyl peroxide] 6×10^{-2} M, [^{t}BuOOH] 7.3×10^{-3} M, [NaClO] 1×10^{-4} M, and [H_2O_2] 1×10^{-2} M. Arrows indicate to which horizontal axis the traces correspond.

Downloaded by [Mizoram University] at 14:40 28 December 2015

Comparable reactivities were observed for benzoyl peroxide and *tert*-butylhydroperoxide. The least reactive was *tert*-butylperoxide. The most noticeable feature of the data in figure 2 is however the following. Though kinetic curves for all oxidants other than ^{t}BuOOH look normal, i.e. the rate of formation of **2** becomes lower with time as the degree of conversion increases, the kinetic curve in the case of *tert*-butylhydroperoxide contains features reminding of a self-accelerating autocatalytic process. Moreover, it is not classical, textbook autocatalysis [39], because the reaction rate continues to increase until the reaction stops completely. Note that the highest rate of formation of **2** is registered during the final stage of the reaction just before its complete halt. Such kinetic curves were not observed for any of the other oxidants studied and the initial rate was always the highest. The challenging difference implied that the mechanism of the **2** → **3** oxidation by *tert*-butylhydroperoxide deserved special attention. Therefore, the organic products formed and kinetics of the reaction of **2** with ^{t}BuOOH were further investigated.

3.2. *^{1}H NMR investigation of the products of reduction of tert-butylhydroperoxide by 1*

The ^{1}H NMR technique has been used for assaying organic fragments produced from ^{t}BuOOH during oxidation of **1** into **2**, which occurs in *ca.* 90% yield (table 1). The spectra of ^{t}BuOOH without **1** (paramagnetic **1** causes line broadening) and with **2** (the diamagnetic μ-oxo dimer) after the completion of the reaction presented in figure 3 show almost quantitative exhaustion of ^{t}BuOOH (δ 1.18) which collapses into ^{t}BuOH (δ 1.17 and 2.41) and acetone (δ 2.09) in 41 and 37% yield, respectively, equation (1). Smaller peaks at δ 1.21, 1.36, and 1.79, the integral intensities of which equal 1, 2, and 2, respectively, arise from three different methyl groups of **2** in the same 1 : 2 : 2 ratio [30]. A smaller peak at δ 3.29 shows that methanol is produced, albeit in lower yield than acetone or ^{t}BuOH. The

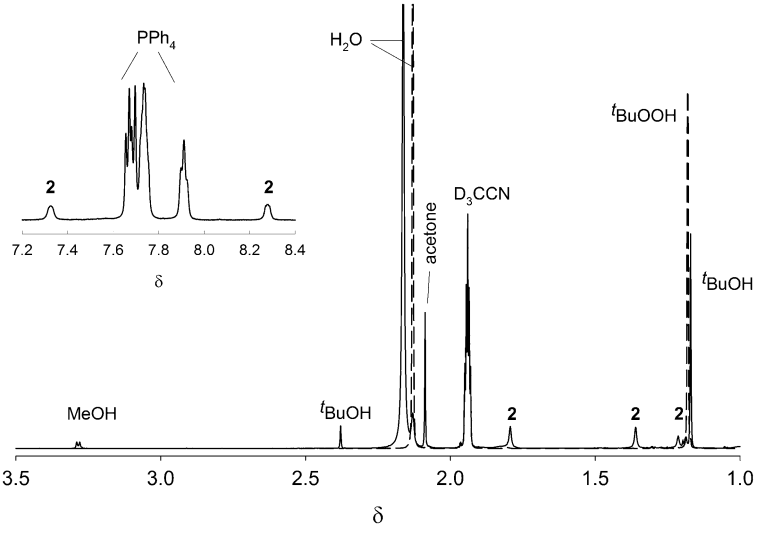

Figure 3. The ^{1}H NMR spectra of ^{t}BuOOH alone (dashed line) and after its reaction with **1** to afford **2** and smaller organic fragments (solid line) in D_3CCN with 0.2% D_2O. Conditions: [^{t}BuOOH] 7.32×10^{-3} M and [**1**] 2.0×10^{-3} M.

spectrum of organic fragments formed, particularly the accumulation of acetone and methanol, is evidence for a free radical character of the reaction between **1** and ^{t}BuOOH. It should also be mentioned that sharp lines in spectrum of products in figure 3 agree with complete conversion of **1** to **2** which eliminates the paramagnetic species in the reaction medium.

$$\mathbf{1} + (H_3C)_3COOH \rightarrow \underset{100\%}{\mathbf{2}} + \underset{41\%}{(H_3C)_3COH} + \underset{37\%}{(H_3C)_2CO} + \underset{13\%}{H_3COH} \quad (1)$$

3.3. *Kinetics of the 1 → 2 oxidation by tert-butylhydroperoxide*

Representative kinetic curves of the generation of **2** from **1** and ^{t}BuOOH obtained in the presence of O_2 (figure 4) are rare and efforts to explore them more thoroughly were made. Their curvature was unusually parabolic, and initial rates were lower than rates measured at any time (t) in many cases provided $t > 0$ and, correspondingly, there was no possibility to estimate the steady-state rates [39]. Moreover, the reaction between **1** and ^{t}BuOOH was light-sensitive. The effect was established by changing the scanning frequency while monitoring the oxidation of **1** with a photodiode array UV–vis spectrometer. The process was noticeably faster when spectra were registered more frequently, i.e. when the time between recording (TbR) of successive spectra was lower (figure 4). The photodiode array instrument releases an undispersed light beam in the 190–1100 nm spectral region and this is the reason for the acceleration displayed in figure 4. The processes subject to "the diode array acceleration" are known and have recently been reviewed [40]. They often occur in the presence of O_2, and their mechanisms which involve radicals are complex though these reactions do not involve species in long-lived excited states.

The reaction kinetics changes noticeably in the absence of O_2 (figure 4). The "parabolicity" vanishes, a noticeable lag period followed by the steady-state portion is observed and

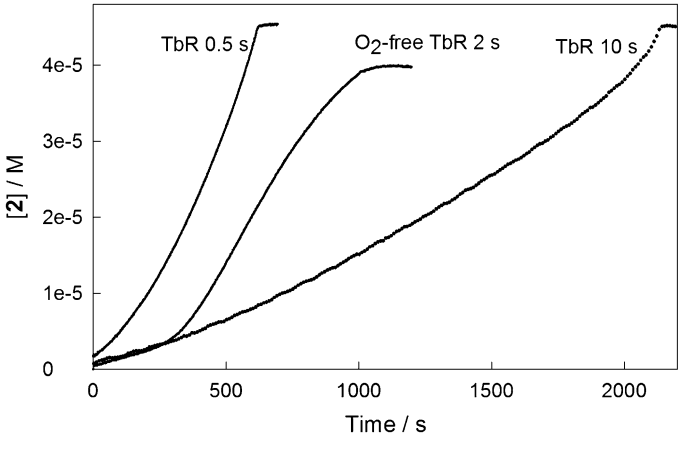

Figure 4. Kinetic curves for the formation of **2** from **1** and ^{t}BuOOH under different conditions: in the absence and in the presence of O_2 and applying different times between scans (different TbR, see text for details). Conditions: MeCN with 0.2% H_2O, −40 °C.

Downloaded by [Mizoram University] at 14:40 28 December 2015

Downloaded by [Mizoram University] at 14:40 28 December 2015

the reaction rate becomes lower as the conversion grows. Thus, O_2 plays a significant role in the reaction consistent with a free radical mechanism. This was further proved by adding 2,2,6,6-tetramethylpiperidine 1-oxyl (tempo), a radical scavenger [41], to the reaction mixture. No formation of **2** was observed in the presence of 1.0×10^{-2} M tempo.

Attempts were made to compare both initial and maximal rates (when the reactions are practically complete) with the concentrations of the reagents **1** and ^{t}BuOOH in the aerated solutions. Figure 5(A) shows that both the initial and maximal rates are virtually independent of [**1**] in the range of $(0.25–5.0) \times 10^{-5}$ M. This, at least qualitatively, helps to understand the origin of the complex kinetic curves of the formation in the case of ^{t}BuOOH presented in figures 2 and 5. In contrast, both the initial and maximal rates depend linearly on [^{t}BuOOH]. The results in figure 5 suggest that the primary role in determining the overall rate of conversion of **1** into **2** belongs to ^{t}BuOOH, which is the key reagent during the initiation and propagation steps.

Recently, Nishida, *et al*. found that proton acceptors accelerate the formation of non-heme Fe^{IV}-oxo complexes from the corresponding Fe^{III} species and $[Ru(bpy)_3]^{3+}$ in aqueous MeCN [42]. Though ^{t}BuOOH is a strikingly different oxidizing agent than Ru^{III}, we thought it might be interesting to test some acids and bases in our system. Bases were of particular interest because they inhibit free radical oxidations [43]. Therefore, the influence of additives shown in table 2 on the kinetics of oxidation of **1** by ^{t}BuOOH was studied.

Hydrogen donors, viz. ^{t}BuOH and MeCOOH, did not affect the kinetics of formation of **2** at all when used at concentrations in excess of both **1** and ^{t}BuOOH. The effect of nitrogen bases was diverse. Most of them (see table 2) stopped the reaction completely and the formation of **2** was not observed. The more sterically congested dabco caused significant rate retardation. Rather unexpectedly, sterically restricted amine tmpp appeared to be a quite remarkable catalyst (figure 6(A)). Higher loadings of tmpp increase the speed of formation of **2,** though the steady-state rate starts to level-off at [tmpp] > 1.0×10^{-2} M. The inset to figure 6(A) compares the kinetics of formation of **2** in the absence and in the presence of

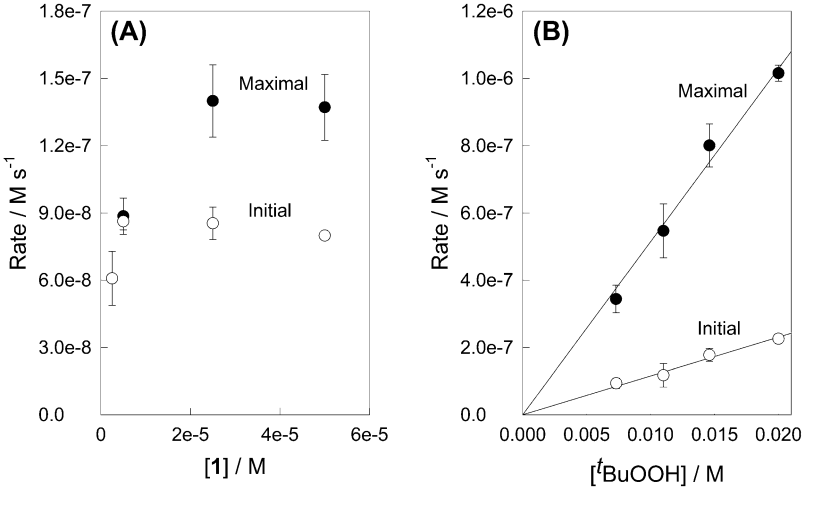

Figure 5. Initial and maximal rates of the reaction between **1** and ^{t}BuOOH as functions of concentrations of **1** (A) and ^{t}BuOOH (B). Other conditions: MeCN with 0.2% H_2O, −40 °C; (A): [^{t}BuOOH] 5.0×10^{-3} M; (B): [**1**] 1.0×10^{-4} M.

Table 2. Influence of effectors on the oxidation of **1** by ^{t}BuOOH in wet MeCN at −40 °C.

Effector	Concentration, M	Effect on **1** + ^{t}BuOOH
1,8-Bis(dimethylamino)naphthalene (proton sponge)	0.010	No reaction
Potassium *tert*-butoxide[a]	7.3×10^{-3}	No reaction
Sodium bis(trimethylsilyl)amide	2.5×10^{-3}	No reaction
Triethylamine	7.3×10^{-3}	No reaction
1,4-Diazabicyclo[2.2.2]octane (dabco)	$(2.5–250) \times 10^{-4}$	Strong retardation
2,2,6,6-Tetramethylpiperidine (tmpp)	$(1–100) \times 10^{-4}$	Acceleration
tert-Butanol	0.025	No effect
Acetic acid	0.025	No effect

[a]Solubilized in the presence of 7.3×10^{-3} M 18-crown-6.

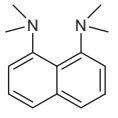

Proton sponge

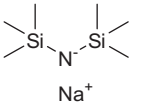

Sodium bis(trimethylsilyl)amide

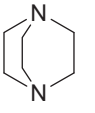

dabco

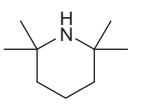

tmpp

5×10^{-4} M tmpp. Tmpp increases the initial and the maximal reaction rate by a factor of 40 and 10, respectively. Moreover, the reaction speed became unaffected by light (similar rate at TbR in the range of 0.5–10 s) and remained practically unchanged during the entire conversion of **1** into **2** implying that the reaction was zero order in **1**. The zero-order hypothesis did not agree with the observation that the slopes of the "zero order" traces appeared to be proportional to the concentration of **1** (figure 6(B)). As in the absence of tmpp, the reaction remained a first-order process in ^{t}BuOOH (figure 6(B)).

The diverse effect of bases (B) is presumably due to their diverse ability to bind to iron (III) of **1**. Amines bind to iron(III) of TAML activators even in water [44] causing minor spectral changes in the UV–vis region. Complexes of the FeB and FeB_2 types are produced blocking the axial sites of the iron polyhedron. The stability of the complexes depends on the nature of the amine [44]. We assume that the blocking of the axial sites prohibits the Fe^{III} to Fe^{IV} oxidation. When the amine nitrogen is sterically protected from binding to iron

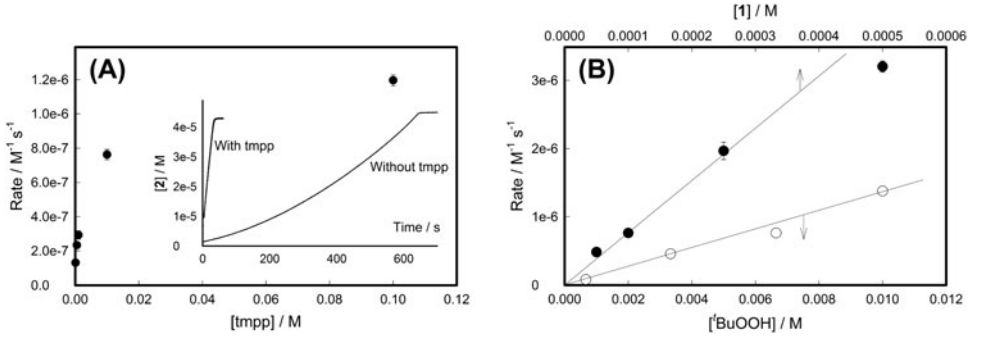

Figure 6. Rates of formation of **2** as functions of [tmpp] (A), [**1**] and [^{t}BuOOH] (both B, arrows indicate to which axis the plot refers). Inset to figure 6(A) shows kinetic curves for formation of **2** with (5.0×10^{-4} M) and without tmpp. Conditions: (A) [**1**] 1.0×10^{-4} M, [^{t}BuOOH] 7.32×10^{-3} M, (inset: [tmpp] 5×10^{-4} M); (B) (variable ^{t}BuOOH): [**1**] 1.0×10^{-4} M, [tmpp] 1.0×10^{-3} M; B (variable **1**) [^{t}BuOOH] 6.7×10^{-3} M, [tmpp] 1.0×10^{-2} M; acetonitrile with 0.2% H_2O, −40 °C.

Downloaded by [Mizoram University] at 14:40 28 December 2015

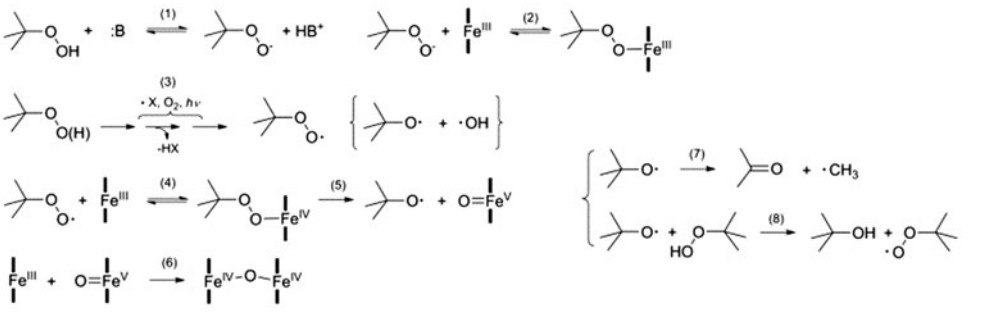

Scheme 1. Tentative mechanistic description of the free radical oxidation of **1** into **2** by ^{t}BuOOH in wet MeCN at −40 °C.

Downloaded by [Mizoram University] at 14:40 28 December 2015

(III) as in the case of tmpp, the mechanism of retardation suggested is turned off and tmpp starts to accelerate the reaction by probably changing the activation mechanism through the deprotonation of ^{t}BuOOH (scheme 1). In the absence of base, the reaction occurs as a free radical, possibly branched, process where light-induced O_2-dependent activation of ^{t}BuOOH may lead to ^{t}BuOO· and/or ^{t}BuO· and ·OH via step 3. The produced ^{t}BuOO· radical reacts in a fast step with Fe^{III} (step 4) to afford the alkylperoxide complex of Fe^{IV}, which undergoes homolytic scission to afford ^{t}BuO· and Fe^{V}oxo complex (step 5). The final product **2** is produced through comproportionation (step 6). The intimate details of the postulated initiation step 3 involving homolytic transformation/s of ^{t}BuOOH are not fully understood. It is likely that the "active" amine (tmpp) eliminates the sensitivity to light by deprotonating ^{t}BuOOH (step 1) and opening the channel for the formation of the alkylperoxide complex of Fe^{III} (step 2), which collapses to the same product as in step 5 through the heterolysis of the O–O bond. Although amines B other than tmpp may also deprotonate ^{t}BuOOH (step 1), the binding of ^{t}BuOO^{-} to iron(III) is precluded due to the generation of unreactive FeB and FeB_2 species with the blocked axial sites.

Steps 7 and 8, which are typical of free radical transformations [45], account for the formation of organic products, namely ^{t}BuOH, acetone and methanol. Minor quantities of MeOH are likely produced via the recombination of methyl and hydroxo radicals (the latter are presumably generated through step 3). We are completely aware of the fact that the true mechanism of the reaction studied may contain additional important steps.

4. Conclusion

This study shows that the oxidation of iron(III) of TAMLs by different oxidizing agents in wet MeCN at −40 °C does not necessarily lead to iron(V) derivatives. More commonly the iron(IV) species are produced. Thus, one should be careful in terms of postulating the Fe^{IV} or Fe^{V} intermediates in TAML-catalyzed oxidative transformations because the highest oxidation state achieved depends crucially on the nature of oxidants used. It is more natural to anticipate the formation of Fe^{V}oxo species when *m*-chloroperoxybenzoic acid or hypochlorite is used. Hydrogen peroxide and common organic peroxides do not allow **1** to reach the oxidation state V, and diiron(IV)-μ-oxo dimers are the more anticipated products.

The nature of peroxide plays a crucial role in determining the reaction mechanism in the organic medium. The unusual kinetics presented here is an evidence for a free radical homolytic mechanism of formation of iron(IV) from *tert*-butylhydroperoxide in MeCN at −40 °C, though ^{t}BuOOH has a tendency to react via a heterolytic mechanism in water under ambient conditions [22]. Interestingly, no unusual kinetics was observed with other peroxides including H_2O_2. This mechanistic difference allows to rationalize two reactivity trends observed in MeCN at −40 °C (^{t}BuOOH > benzoyl peroxide > H_2O_2) *versus* that observed in water at 25 °C (benzoyl peroxide > H_2O_2 > ^{t}BuOOH) [26] – free radical and heterolytic mechanisms are realized for ^{t}BuOOH in the organic solvent and in water, respectively.

Downloaded by [Mizoram University] at 14:40 28 December 2015

Acknowledgments

Operating support is acknowledged from the Heinz Endowments (T.J.C.), and the Environmental Protection Agency (grant RD 83 to T.J.C.) and the Steinbrenner Institute for a Steinbrenner Institute Graduate Fellowship. NMR instrumentation at CMU was partially supported by NSF (CHE-0130903 and CHE-1039870). The authors thank Dr Karla Arias-Salazar and Dr Soumen Kundu for guidance in the development of this project.

Disclosure statement

No potential conflict of interest was reported by the authors.

Funding

This work was supported by the Environmental Protection Agency [grant number RD 83] and the Steinbrenner Institute for a Steinbrenner Institute Graduate Fellowship. NMR instrumentation at CMU was partially supported by NSF [grant number CHE-0130903], [grant number CHE-1039870].

References

[1] I. Bertini, H.B. Gray, S.J. Lippard, J.S. Valentine. *Bioinorganic Chemistry*, University Science Books, Mill Valley, CA (1994).
[2] B. Meunier. *Biomimetic Oxidations Catalyzed by Transition Metal Complexes*, Imperial College Press, London (2000).
[3] S.J. Lippard, J.M. Berg (Eds.). *Principles of Bioinorganic Chemistry*, University Science Books, Sausalito, CA (1994).
[4] B. Meunier. *Models of Heme Peroxidases and Catalases*, Imperial College Press, London (2000).
[5] B. Meunier, S.P. de Visser, S. Shaik. *Chem. Rev.*, **104**, 3947 (2004).
[6] P.R. Ortiz de Montelano (Ed.). *Cytochrome P450 Structure, Mechanism, and Biochemistry*, Kluwer Academic/Plenum Publishers, New York (2005).
[7] S. Shaik, D. Kumar, S.P. de Visser, A. Altun, W. Thiel. *Chem. Rev.*, **105**, 2279 (2005).
[8] I. Bertini, H.B. Gray, E.I. Stiefel, J.S. Valentine. *Biological Inorganic Chemistry. Structure and Reactivity*, University Science Books, Sausalito, CA (2007).
[9] L. Que. *Acc. Chem. Res.*, **40**, 493 (2007).
[10] W. Nam, Y.-M. Lee, S. Fukuzumi. *Acc. Chem. Res.*, **47**, 1146 (2014).
[11] A.R. McDonald, L. Que. *Coord. Chem. Rev.*, **257**, 414 (2014).
[12] R. Van Eldik, C. Ducker-Benfer, F. Thaler. *Adv. Inorg. Chem.*, **49**, 1 (2000).
[13] C. Fertinger, A. Franke, R. van Eldik. *J. Biol. Inorg. Chem.*, **17**, 27 (2012).

[14] M. Oszajca, A. Drzewiecka-Matuszek, A. Franke, D. Rutkowska-Zbik, M. Brindell, M. Witko, G. Stochel, R. van Eldik. *Chem. Eur. J.*, **20**, 2328 (2014).
[15] L. Ji, A. Franke, M. Brindell, M. Oszajca, A. Zahl, R. van Eldik. *Chem. Eur. J.*, **20**, 14437 (2014).
[16] C. Fertinger, N. Hessenauer-Ilicheva, A. Franke, R. van Eldik. *Chem. Eur. J.*, **15**, 13435 (2009).
[17] T.J. Collins. *Acc. Chem. Res.*, **27**, 279 (1994).
[18] T.J. Collins. *Acc. Chem. Res.*, **35**, 782 (2002).
[19] T.J. Collins, S.K. Khetan, A.D. Ryabov. In *Handbook of Green Chemistry*, P.T. Anastas, R.H. Crabtree (Ed.), pp. 39–77, Wiley-VCH Verlag GmbH & KgaA, Weinheim (2009).
[20] A.D. Ryabov, T.J. Collins. *Adv. Inorg. Chem.*, **61**, 471 (2009).
[21] A.D. Ryabov. *Adv. Inorg. Chem.*, **65**, 118 (2013).
[22] D.-L. Popescu, M. Vrabel, A. Brausam, P. Madsen, G. Lente, I. Fabian, A.D. Ryabov, R. van Eldik, T.J. Collins. *Inorg. Chem.*, **49**, 11439 (2010).
[23] S. Sen Gupta, M. Stadler, C.A. Noser, A. Ghosh, B. Steinhoff, D. Lenoir, C.P. Horwitz, K.-W. Schramm, T.J. Collins. *Science*, **296**, 326 (2002).
[24] A. Chanda, S.K. Khetan, D. Banerjee, A. Ghosh, T.J. Collins. *J. Am. Chem. Soc.*, **128**, 12058 (2006).
[25] D. Banerjee, A.L. Markley, T. Yano, A. Ghosh, P.B. Berget, E.G. Minkley Jr., S.K. Khetan, T.J. Collins. *Angew. Chem. Int. Ed.*, **45**, 3974 (2006).
[26] N. Chahbane, D.-L. Popescu, D.A. Mitchell, A. Chanda, D. Lenoir, A.D. Ryabov, K.-W. Schramm, T.J. Collins. *Green Chem.*, **9**, 49 (2007).
[27] N.W. Shappell, M.A. Vrabel, P.J. Madsen, G. Harrington, L.O. Billey, H. Hakk, G.L. Larsen, E.S. Beach, C.P. Horwitz, K. Ro, P.G. Hunt, T.J. Collins. *Environ. Sci. Technol.*, **42**, 1296 (2008).
[28] S. Kundu, A. Chanda, L. Espinosa-Marvan, S.K. Khetan, T.J. Collins. *Catal. Sci. Technol.*, **2**, 1075 (2012).
[29] S. Hong, K.D. Sutherlin, J. Park, E. Kwon, M.A. Siegler, E.I. Solomon, W. Nam. *Nat. Commun.*, 5 (2014).
[30] A. Ghosh, F. Tiago de Oliveira, T. Toshihiro Yano, T. Nishioka, E.S. Beach, I. Kinoshita, E. Münck, A.D. Ryabov, C.P. Horwits, T.J. Collins. *J. Am. Chem. Soc.*, **127**, 2505 (2005).
[31] F. Tiago de Oliveira, A. Chanda, D. Banerjee, X. Shan, S. Mondal, L. Que J., E.L. Bominaar, E. Munck, T.J. Collins. *Science*, **315**, 835 (2007).
[32] S. Kundu, J. Van Kirk Thompson, A.D. Ryabov, T.J. Collins. *J. Am. Chem. Soc.*, **133**, 18546 (2011).
[33] D.D. Do Pham, G.F. Kelso, Y. Yang, M.T.W. Hearn. *Green Chem.*, **16**, 1399 (2014).
[34] R. Li, G. Wang, Y. Liu, X. Chen, Z. Sun, H. Liu, X. Wang, Z. Wu, Z. Liu. *Appl. Mech. Mater.*, **723**, 601 (2015).
[35] F. Napoly, R. Kieffer, L. Jean-Gérard, C. Goux-Henry, M. Draye, B. Andrioletti. *Tetrahedron Lett.*, **56**, 2517 (2015).
[36] D.D. Do Pham, G.F. Kelso, Y. Yang, M.T.W. Hearn. *Green Chem.*, **14**, 1189 (2012).
[37] J.G. Hill, B.E. Rossiter, K.B. Sharpless. *J. Org. Chem.*, **48**, 3607 (1983).
[38] M.J. Bartos, S.W. Gordon-Wylie, B.G. Fox, L.J. Wright, S.T. Weintraub, K.E. Kauffmann, E. Münck, K.L. Kostka, E.S. Uffelman, C.E.F. Rickard, K.R. Noon, T.J. Collins. *Coord. Chem. Rev.*, **174**, 361 (1998).
[39] J.H. Espenson. *Chemical Kinetics and Reaction Mechanisms*, McGraw-Hill Inc., New York (1995).
[40] I. Fabian, G. Lente. *Pure Appl. Chem.*, **82**, 1957 (2010).
[41] V.W. Bowry, K.U. Ingold. *J. Am. Chem. Soc.*, **114**, 4992 (1992).
[42] Y. Nishida, Y. Morimoto, Y.-M. Lee, W. Nam, S. Fukuzumi. *Inorg. Chem.*, **52**, 3094 (2013).
[43] I.V. Berezin, E.T. Denisov, N.M. Emanuel. *The Oxidation of Cyclohexane*, Pergamon, Oxford (1966).
[44] V. Polshin, D.-L. Popescu, A. Fischer, A. Chanda, D.C. Horner, E.S. Beach, J. Henry, Y.-L. Qian, C.P. Horwitz, G. Lente, I. Fabian, E. Münck, E.L. Bominaar, A.D. Ryabov, T.J. Collins. *J. Am. Chem. Soc.*, **130**, 4497 (2008).
[45] J.K. Kochi. *J. Am. Chem. Soc.*, **84**, 1193 (1962).

Downloaded by [Mizoram University] at 14:40 28 December 2015